This article has been accepted for publication in a future issue of this journal, but has not been fully edited. Content may change prior to final publication. Citation information: DOI 10.1109/TWC.2014.2317788, IEEE Transactions on Wireless Communications

Equal Gain Combining for Cooperative Spectrum Sensing in Cognitive Radio Networks

Doha Hamza, *Student Member, IEEE*, Sonia Aïssa, *Senior Member, IEEE*, Ghassane Aniba, *Member, IEEE*

***Abstract*—Sensing with equal gain combining (SEGC), a novel cooperative spectrum sensing technique for cognitive radio networks, is proposed. Cognitive radios simultaneously transmit their sensing results to the fusion center (FC) over multipath fading reporting channels. The cognitive radios estimate the phases of the reporting channels and use those estimates for coherent combining of the sensing results at the FC. A global decision is made at the FC by comparing the received signal with a threshold. We obtain the global detection probabilities and secondary throughput exactly through a moment generating function approach. We verify our solution via system simulation and demonstrate that the Chernoff bound and central limit theory approximation are not tight. The cases of hard sensing and soft sensing are considered and we provide examples in which hard sensing is advantageous to soft sensing. We contrast the performance of SEGC with maximum ratio combining of the sensors' results and provide examples where the former is superior. Furthermore, we evaluate the performance of SEGC against existing orthogonal reporting techniques such as time division multiple access (TDMA). SEGC performance always dominates that of TDMA in terms of secondary throughput. We also study the impact of phase and synchronization errors and demonstrate the robustness of the SEGC technique against such imperfections.**

***Index Terms*—Cognitive radio networks, equal gain combining, maximum ratio combining, soft sensing, hard sensing.**

I. Introduction

Spectrum sensing is one of the key enabling technologies for cognitive radios. To achieve a specified detection performance, despite heavy shadowing and fading, cooperative spectrum sensing was proposed as an effective way to reliably detect primary activity [1]–[4]. Cooperation is achieved by allowing different secondary users to share their sensing results, usually via a central node or fusion center (FC), which makes a global decision on the occupancy status of the licensed band.

The local sensors typically transmit sensing information to the FC through orthogonal channels, for example using time division multiple access (TDMA) or frequency division multiple access (FDMA). The TDMA approach does not suit the cognitive setting because significant delay and throughput loss occur as the number of sensors increase. On the hand, the use of FDMA through sending the decisions on orthogonal frequency bands requires a large bandwidth [5]. These issues contradict the basic premise of cognitive radios in which the terminals search for transmission opportunities and can only communicate with the FC through a low-rate reporting channel with a limited bandwidth.

In order to address this issue of efficiently reporting the sensing results to the FC, simultaneous transmission by the local sensors was considered in [6]–[9]. In [6], the FC collects data in multiple slots, each involving a random number of transmitting sensors. Specifically, sensors with the same data value transmit (if they decide to do so) using the same waveform on a multi-access fading channel, and the design criterion is to find the optimal mean transmission rate so that the detection error exponent is maximized. The use of orthogonal waveforms eliminates interference among sensors with different data values and makes it possible to have a coherent combining of transmissions. This, however, happens only in the absence of channel fading. In [7], each sensor makes a binary local decision and communicates it to the FC simultaneously with the other sensors. The authors investigate the detection performance in terms of the error probability and error exponent for Rayleigh and Rician fading scenarios. The communication is assumed to be non-coherent, meaning that the channel gains are unknown at both the sensors and the FC. Furthermore, detection errors, whether a false alarm or a miss-detection, are therein assumed to have an equal impact and henceforth combined in a single error term, which may not suit cognitive networks since the two users, namely the primary and the secondary, will be impacted differently by the false alarm and miss-detection events.

Reference [8] also considers the simultaneous transmission of sensors' decisions in a wireless sensor network (WSN). Non-coherent combining is studied with average energy constraints. Because of the WSN setting, a weighted sum of the false alarm and the miss-detection probabilities is also combined in a single error term which is not suitable in cognitive networks as argued above. A soft sensing technique is considered in [9], where simultaneous transmission is used with maximum ratio combining (MRC) of the sensing results. This requires the knowledge of the reporting channel's phase and magnitude at each local sensor. Furthermore, the authors solve for the achievable detection performance using a central limit theorem (CLT) approximation.

In this paper, we also consider the simultaneous transmission of the sensing results from all the cognitive radios (CRs) to the FC over fading reporting channels, and propose a novel cooperative sensing scheme, termed *sensing with equal gain combining* (SEGC). Under our model, each CR dephases its transmitted signal and equal gain combining of the sensors'

Manuscript received September, 3, 2013; revised December, 25, 2013 and March 30, 2014; accepted March, 30, 2014. The review of this paper was coordinated by M. Elkashlan.

D. Hamza is with the Computer, Electrical and Mathematical Sciences & Engineering (CEMSE) Division, King Abdullah University of Science and Technology (KAUST), Thuwal, KSA (e-mail: doha.hamzamohamed@kaust.edu.sa).

S. Aïssa is with the Institut National de la Recherche Scientifique (INRS), University of Quebec, Montreal, QC, Canada (email: aissa@emt.inrs.ca).

G. Aniba is with Ecole Mohammadia d'Ingénieurs (EMI), Université Mohammed V Agdal (UM5A), Rabat, Morocco (email: ghassane@emi.ac.ma).

This article has been accepted for publication in a future issue of this journal, but has not been fully edited. Content may change prior to final publication. Citation information: DOI 10.1109/TWC.2014.2317788, IEEE Transactions on Wireless Communications

decisions is implemented at the FC. Relative to previous work, the contributions of this work are as follows:

i) We obtain the exact values of the global false alarm and miss-detection probabilities for the proposed SEGC technique by deriving the moment generating function (MGF) for the received signal at the FC. Our scheme can be efficiently implemented using the fast Fourier transform (FFT). While a Rayleigh fading distribution is assumed for the reporting channels between the CRs and the FC, this choice of distribution is not critical to the success of our scheme which can be extended to any general fading distribution, provided that the MGF for the received signal at the FC exists.

ii) In addition to quantifying the detection error probabilities, we also consider the secondary throughput as a performance metric. While detection error probabilities can be reduced by increasing the sensing time, this comes at the expense of reducing the transmission time, and hence the throughput, of the secondary user. This is the essence of the sensing-throughput tradeoff in cognitive radio networks [10].

iii) We demonstrate communication scenarios where equal gain combining of sensors' decisions is superior to MRC, which is used in [9]. Our results are in harmony with other work in the literature, e.g. [11], [12], which show that MRC receivers may be optimal in a data transmission diversity context, but not necessarily so in a decentralized detection setup. The proposed SEGC technique also has a practical advantage over MRC since the transmitted waveform has a constant envelope. This allows radio power amplifiers to operate at maximum efficiency [13].[1]

iv) We show the advantage of hard sensing over soft sensing under certain transmission conditions, specifically when the signal-to-noise ratio (SNR) is sufficiently high. Although previous work, e.g. [17], shows a clear advantage for soft sensing over hard sensing in the presence of reporting channel errors, the result is confined to the orthogonal reporting of sensing results.[2] To the best of our knowledge, no study exists on the difference between soft sensing and hard sensing when simultaneous reporting of sensors' results is employed.

v) We also investigate the impact of realistic errors, such as phase and synchronization errors, and demonstrate the robustness of the proposed SEGC to such errors.

vi) We demonstrate that the Chernoff bound is not tight in our setup. Further, the CLT approximation, which is considered in [9], is shown not to be accurate when the local sensing time is small and when the number of sensors is small. Hence, an exact computation of the collaborative sensing performance is needed.

[1]It is important to note that EGC schemes are also considered in [11], [12], [14]–[16]. However, therein the sensors' decisions are reported in an orthogonal fashion and not simultaneously.

[2]Note that within the realm of orthogonal reporting of sensors' decisions, the work in [18] shows an advantage of hard sensing over soft sensing from the detection probabilities' point of view, although the result is achieved using sequential detection and perfect reporting.

N	Number of cognitive radios in the network
CR_n	A given cognitive radio in the network
FC	Fusion center
y	Received signal at the FC
v_n	Local decision/value transmitted by CR_n to the FC
h_n	Complex channel gain between CR_n and FC, with magnitude $\lvert h_n\rvert$ and phase θ_n
ϵ	FC receiver zero-mean Gaussian noise with variance σ^2
w_n	Weight factor used by CR_n to multiply its decision
$\mathcal{H}_0$	Null hypothesis (idle PU)
$\mathcal{H}_1$	Alternative hypothesis (active PU)
Q_{f}	Global false alarm probability for the SEGC scheme
Q_{m}	Global miss-detection probability for the SEGC scheme
$Q_{\mathrm{f,TDMA}}$	Global false alarm probability for the TDMA scheme
$Q_{\mathrm{m}}^{(\mathrm{T})}$	Primary network maximum miss-detection threshold
$p_{\mathrm{f},n}$	Local false alarm probability at CR_n
$p_{\mathrm{d},n}$	Local detection probability at CR_n
λ	Global decision threshold at the FC
λ_n	Local decision threshold at CR_n
α_n	Rayleigh fading parameter for $\lvert h_n\rvert$
u	Time-bandwidth product
$\gamma_{\mathrm{s},n}$	Sensing channel SNR between the PU and CR_n
$\bar{\gamma}_{\mathrm{s},n}$	Average sensing channel SNR between the PU and CR_n
$\gamma_{\mathrm{r},n}$	Reporting channel SNR between CR_n and FC
$\bar{\gamma}_{\mathrm{r},n}$	Average reporting channel SNR between CR_n and FC
γ	Energy used by the FC to send the pilot signal
$\hat{\theta}_n$	ML estimator of the phase of the channel between FC and CR_n
$\delta\theta_n$	Difference between true channel phase and estimated phase for CR_n
$Y_{\mathrm{I},n}/Y_{\mathrm{Q},n}$	In-phase/Quadrature received signals at CR_n
$\epsilon_{\mathrm{I},n}/\epsilon_{\mathrm{Q},n}$	In-phase/Quadrature receiver noise each distributed as $\mathcal{N}(0,\sigma_n^2)$
ϵ_n	FC receiver zero-mean Gaussian noise in the nth mini-slot with variance σ^2
T	Time slot duration
τ	Time taken by the CRs to send their sensing decisions
τ_s	Time used by the CRs for local sensing
r_s	Mean secondary transmission rate
η_n	Timing error between the FC and CR_n
$Q(.)$	Tail probability of the standard normal distribution
$\Gamma_{\mathrm{inc}}(.,.)$	Normalized incomplete Gamma function
$\mathrm{erf}(.)$	The error function

TABLE I
LIST OF THE MAIN SYMBOLS USED IN THE PAPER.

In the next section we detail the system model with a focus on the hard sensing case. In Section III, we study the impact of using soft sensing information and of having errors in phase estimation. Then, in Section IV, we present some numerical results and, finally, we conclude the paper in Section V. A list of the symbols and special functions used is provided in Table I.

II. COLLABORATIVE SENSING WITH EQUAL GAIN COMBINING

We consider a primary channel that operates in a time-slotted manner. Primary activity over the channel changes independently from one slot to another. A cognitive network of N CRs coexists with the primary and tries to opportunistically access the primary channel when it is free. To realize this objective, the cognitive nodes carry out spectrum sensing at the beginning of each time slot, and then either make a binary decision on the state of primary activity and send it to the FC, called hard sensing, or directly transmit the received sensing power or energy to the FC, called soft sensing. In either case, a given cognitive radio (CR_n) transmits a decision/value v_n to the FC. For the rest of this section, we focus on the hard sensing case. The soft sensing case is treated in Section III.

Communication with the FC takes place over low-rate fading channels with limited bandwidth. The reporting channels

This article has been accepted for publication in a future issue of this journal, but has not been fully edited. Content may change prior to final publication. Citation information: DOI 10.1109/TWC.2014.2317788, IEEE Transactions on Wireless Communications

function in a time division duplexing (TDD) fashion, which means that both directions of communication, from the radios to the FC and from the FC to the radios, operate using the same carrier frequency. The coherence time of the sensing and reporting channels is assumed to span many time slots. Channel estimation is performed periodically to track the channel variations. Specifically, the FC sends a pilot signal to all cognitive nodes. This pilot signal is used by each CR_n ($n = 1, \cdots, N$) to estimate the phase introduced by the fading channel between itself and the FC. At the beginning of each time slot, each CR_n performs spectrum sensing of the wireless medium to make a binary decision regarding the presence of the primary user (PU). All CRs then use ON/OFF keying (OOK) to *simultaneously* signal back to the FC the status of the PU. To allow for a coherent addition of the received signals at the FC, each CR_n dephases its signal by multiplying it with the phase estimate obtained from the earlier FC pilot signal.

In this section, we assume that the phase estimates are perfect and we derive the performance metrics for the proposed SEGC scheme accordingly. We account for errors in the phase estimates in Section III-B.

A. Statistics of the Received Signal at the FC

Based on the described model, we have the following received signal at the FC

$$y = \sum_{n=1}^{N} w_n^* h_n v_n + \epsilon, \tag{1}$$

where $h_n = |h_n| e^{i\theta_n}$ (with magnitude $|h_n|$ and phase θ_n) is the complex channel gain between CR_n and the FC, and v_n is the local (hard) decision made by CR_n regarding the primary activity: $v_n = 0$ if the PU is sensed to be idle and $v_n = 1$ if it is sensed to be active.[3] The term $\epsilon \sim \mathcal{N}(0, \sigma^2)$ is the receiver zero-mean Gaussian noise at the FC with variance σ^2, parameter w_n is the weight factor used by the n^{th} sensor to multiply its decision, and $(.)^*$ denotes the complex conjugation. For the SEGC scheme, we consider $w_n = e^{i\theta_n}$. Thus, we have

$$y = \sum_{n=1}^{N} |h_n| v_n + \epsilon. \tag{2}$$

In the numerical analysis section, we also consider the MRC scheme, i.e. where w_n is proportional to h_n, and compare its performance with the SEGC scheme. Note that the use of the word EGC in our work should not be confused with its use in a diversity combining communication scheme, where the *same* symbol is sent over multiple antennas in the case of transmit diversity. In our distributed detection setup, possibly different symbols, representing the local decisions at the sensors, are sent over different reporting channels. In adopting the term EGC, we are referring to the fact that the FC's received signal in (2) is similar to the signal obtained via EGC in diversity combining techniques, hence the SEGC terminology.

[3]Note that assuming a direct down-conversion in-phase/quadrature (IQ) receiver [13], we use the received signal on the in-phase branch since there is no signal component on the quadrature branch in the case of perfect channel phase estimates.

We consider the null hypothesis, $\mathcal{H}_0$, to refer to an idle PU. The alternative hypothesis, $\mathcal{H}_1$, refers to an active PU. Under a threshold test on the received signal y, the false alarm and miss-detection probabilities are defined as

$$Q_{\text{f}} = \Pr\left\{ y > \lambda \middle| \mathcal{H}_0 \right\}, \tag{3}$$

$$Q_{\text{m}} = \Pr\left\{ y < \lambda \middle| \mathcal{H}_1 \right\}, \tag{4}$$

where λ is the global decision threshold at the FC. In order to calculate the above probabilities, the probability density functions (PDFs) $f_Y(y|\mathcal{H}_0)$ and $f_Y(y|\mathcal{H}_1)$ need to be found. Assuming independent sensor decisions and independent channel gains, the PDF of the received signal at the FC, conditioned on the sensors' decisions $(v_1, v_2, \cdots, v_N)$, the channel gains $(h_1, h_2, \cdots, h_N)$ and either hypothesis, is Gaussian. That is,

$$\begin{aligned} f_Y\left(y \middle| v_1, ..., v_N, h_1, ..., h_N, \mathcal{H}_\circ\right) &= f_Y\left(y \middle| v_1, ..., v_N, h_1, ..., h_N, \mathcal{H}_1\right) \\ &= \frac{1}{\sqrt{2\pi}\sigma} \exp\left(- \frac{\left[y - \sum_{n=1}^{N} |h_n| v_n \right]^2}{2\sigma^2} \right). \end{aligned} \tag{5}$$

The v_n's are Bernoulli random variables. Thus, under the null hypothesis, we have

$$|h_n| v_n = \begin{cases} |h_n| & \text{w.p. } p_{\text{f},n} \\ 0 & \text{w.p. } 1 - p_{\text{f},n} \end{cases} \tag{6}$$

where $p_{\text{f},n}$ is the local false alarm probability at CR_n, and where w.p. stands for 'with probability'. Using (6) and by averaging over all the possible combinations of the $v_1, v_2, \cdots, v_N$ values, we may write $f(y|h_1, ..., h_N, \mathcal{H}_0)$ as

$$\begin{aligned} &f_Y(y|h_1, ..., h_N, \mathcal{H}_\circ) \\ &= \sum_{v_1, v_2, ..., v_N} \frac{\exp\left(- \frac{\left[y - \sum_{n=1}^{N} |h_n| v_n \right]^2}{2\sigma^2} \right)}{\sqrt{2\pi}\sigma} \prod_{n=1}^{N} p_{\text{f},n}^{v_n} \left(1 - p_{\text{f},n}\right)^{1 - v_n}, \end{aligned} \tag{7}$$

where $\sum_{v_1, v_2, ..., v_N}$ is a summation over all the possible values of the random binary sequence $v_1, v_2, \cdots, v_N$ starting from 00...0 to 11...1. Under hypothesis $\mathcal{H}_1$, it is straightforward to show that

$$\begin{aligned} &f_Y(y|h_1, ..., h_N, \mathcal{H}_1) \\ &= \sum_{v_1, v_2, ..., v_N} \frac{\exp\left(- \frac{\left[y - \sum_{n=1}^{N} |h_n| v_n \right]^2}{2\sigma^2} \right)}{\sqrt{2\pi}\sigma} \prod_{n=1}^{N} p_{\text{d},n}^{v_n} \left(1 - p_{\text{d},n}\right)^{1 - v_n}, \end{aligned} \tag{8}$$

where $p_{\text{d},n}$ is the local detection probability at CR_n.

In our model, we do not assume channel gain knowledge at the FC. This would require feeding back all the channel estimates to the FC, or making the cognitive nodes send pilots to the FC in a one-by-one fashion. In this case, we face the same problems that hinder orthogonal decision reporting such as the bandwidth requirements and the impact on throughput, albeit happening now only when the channel gains need to be updated. For this reason, we restrict channel knowledge at the FC to that of channel gain statistics. The PDFs $f_Y(y|\mathcal{H}_0)$ and $f_Y(y|\mathcal{H}_1)$ should be obtained from (7) and (8) via averaging over all the channel gains. However, there is no closed-form

This article has been accepted for publication in a future issue of this journal, but has not been fully edited. Content may change prior to final publication. Citation information: DOI 10.1109/TWC.2014.2317788, IEEE Transactions on Wireless Communications

expression for $f_Y(y|\mathcal{H}_0)$ and $f_Y(y|\mathcal{H}_1)$ using (7) and (8), respectively, even when considering the simple case of two sensors simultaneously transmitting results. Hence, a different approach is needed which is discussed next.

B. The MGF Approach

Since the PDFs of y conditioned on $\mathcal{H}_0$ or $\mathcal{H}_1$ are difficult to compute analytically, we resort to an efficient way to numerically compute the required probabilities in order to study the performance of the proposed SEGC scheme. The same approach is employed in other works, e.g. [16], [19], where the exact calculation of the detection probabilities is needed. We proceed by computing the MGF of y under the two hypotheses, and then we use the inverse discrete Fourier transform (IDFT) to compute the PDF. We detail the procedure for the MGF of y under the null hypothesis, denoted as $\mathcal{M}_Y^{\mathrm{EGC,HS}}(\rho|\mathcal{H}_0)$,[4] and the corresponding MGF for y under the alternative hypothesis, denoted $\mathcal{M}_Y^{\mathrm{EGC,HS}}(\rho|\mathcal{H}_1)$, follows in the same fashion.

By definition, we have

$$\mathcal{M}_Y^{\mathrm{EGC,HS}}(\rho|\mathcal{H}_0) = \mathbb{E}\left[\exp\left(\rho y\right)|\,\mathcal{H}_0\right], \tag{9}$$

where $\mathbb{E}(.)$ denotes the expectation operator. Using (2) in (9) and under the assumption of independence of all the involved random variables, the MGF can be evaluated as

$$\begin{aligned}\mathcal{M}_Y^{\mathrm{EGC,HS}}(\rho|\mathcal{H}_0) =& \mathbb{E}(\exp\left(\rho\epsilon\right))\mathbb{E}\left[\exp\left(\rho\sum_{n=1}^{N}|h_n|v_n\right)\Big|\mathcal{H}_0\right]\\ =& \exp\left(\frac{1}{2}\rho^2\sigma^2\right)\prod_{n=1}^{N}\mathbb{E}\left[\exp\left(\rho|h_n|v_n\right)|\mathcal{H}_0\right].\end{aligned} \tag{10}$$

Recall that the v_n's are Bernoulli random variables so that $v_n = 1$ w.p. $p_{f,n}$, under the null hypothesis. We also assume a Rayleigh distribution for the random variables $|h_n|$, i.e. the PDF of $|h_n|$ is

$$f(|h_n|) = \frac{|h_n|}{\alpha_n^2}e^{-|h_n|^2/2\alpha_n^2}, \tag{11}$$

where α_n denotes the Rayleigh fading parameter for $|h_n|$. By making use of this information, we obtain,

$$\begin{aligned}\mathcal{M}_Y^{\mathrm{EGC,HS}}(\rho|\mathcal{H}_0) =& \mathbb{E}(\exp\left(\rho\epsilon\right))\mathbb{E}\left[\exp\left(\rho\sum_{n=1}^{N}|h_n|v_n\right)\Big|\mathcal{H}_0\right]\\ =& \exp\left(\frac{1}{2}\rho^2\sigma^2\right)\prod_{n=1}^{N}\mathbb{E}\left[\exp\left(\rho|h_n|v_n\right)|\mathcal{H}_0\right].\end{aligned} \tag{12}$$

where $\mathrm{erf}(.)$ denotes the error function.
Proceeding in a similar way, we also obtain

$$\begin{aligned}&\mathcal{M}_Y^{\mathrm{EGC,HS}}(\rho|\mathcal{H}_1) = \exp\left(\frac{1}{2}\rho^2\sigma^2\right)\\ &\prod_{n=1}^{N}\left(1+\sqrt{\frac{\pi}{2}}p_{\mathrm{d},n}\alpha_n\rho\exp\left(\frac{(\rho\alpha_n)^2}{2}\right)\left[1+\mathrm{erf}\left(\frac{\rho\alpha_n}{\sqrt{2}}\right)\right]\right).\end{aligned} \tag{13}$$

[4]Recall that we focus in this section on the hard sensing case.

Now, using the derived expressions for the MGF, the PDF of y can be evaluated by noting the following relationship:

$$\mathcal{M}_Y^{\mathrm{EGC,HS}}(-i2\pi f|\mathcal{H}_0) = \int_{-\infty}^{\infty} f_Y(y|\mathcal{H}_0)\exp\left(-i2\pi fy\right)dy. \tag{14}$$

This means that $\mathcal{M}_Y^{\mathrm{EGC,HS}}(-i2\pi f|\mathcal{H}_0)$ and $f_Y(y|\mathcal{H}_0)$ form a Fourier transform pair, and hence $f_Y(y|\mathcal{H}_0)$ can be obtained from $\mathcal{M}_Y^{\mathrm{EGC,HS}}(-i2\pi f|\mathcal{H}_0)$ via the IDFT which can be efficiently implemented via variable discretization and use of the inverse fast Fourier transform (IFFT). This method is detailed in [20] and [21], together with an investigation of the accuracy and error bounds. Similarly, $f_Y(y|\mathcal{H}_1)$ can be obtained from $\mathcal{M}_Y^{\mathrm{EGC,HS}}(-i2\pi f|\mathcal{H}_1)$. It is noted in (12) and (13) that an evaluation of the error function with complex arguments is needed. This can be achieved using a series representation of the error function as illustrated in [22].

In the performance analysis section, we will demonstrate the performance of the proposed hard sensing scheme and also contrast it with two modifications to the system model, which are discussed next.

III. SEGC Under Soft Sensing and Estimation Errors

In this section, we consider two different SEGC scenarios. In the first one, instead of each CR sending a binary decision regarding the presence of the PU as treated in the previous section, it instead sends the value of the measured sensing power, i.e. soft sensing is used. In the second scenario, we consider the case when phase errors occur so that the cognitive nodes cannot completely dephase their transmitted signals to the FC. Our goal in addressing these cases is to quantify the difference in performance in using hard versus soft information, and to also study the impact of practical errors, such as errors in phase estimation on the proposed collaborative sensing scheme.

A. Use of Soft Sensing Information

Herein, the setting is identical to the hard sensing model described in Section II except that the v_n's now have the following distribution [23],

$$v_n = \begin{cases}\chi_{2u}^2, & \text{under } \mathcal{H}_0\\ \chi_{2u}^2\left(2\gamma_{\mathrm{s},n}\right), & \text{under } \mathcal{H}_1\end{cases} \tag{15}$$

where u is the time-bandwidth product and $\gamma_{\mathrm{s},n}$ is the sensing channel SNR between the PU and CR$_n$, χ_{2u}^2 is a central Chi-squared random variable with $2u$ degrees of freedom, i.e.

$$f(v_n, 2u) = \frac{v_n^{u-1}e^{-v_n/2}}{2^u\Gamma(u)}, \tag{16}$$

where $\Gamma(a) = \int_0^\infty t^{a-1}\exp\left(-t\right)dt$ is the Gamma function. The variable $\chi_{2u}^2\left(2\gamma_{\mathrm{s},n}\right)$ denotes a non-central Chi-squared random variable with $2u$ degrees of freedom and a non-centrality parameter $2\gamma_{\mathrm{s},n}$, i.e.

$$f(v_n, 2u, 2\gamma_{\mathrm{s},n}) = \sum_{k=0}^{\infty}\frac{e^{-\gamma_{\mathrm{s},n}}\gamma_{\mathrm{s},n}^k}{k!}f(v_n, 2(u+k)). \tag{17}$$

This article has been accepted for publication in a future issue of this journal, but has not been fully edited. Content may change prior to final publication. Citation information: DOI 10.1109/TWC.2014.2317788, IEEE Transactions on Wireless Communications

Proceeding in a similar fashion to the analysis described in the previous section, the MGF under the null and alternative hypotheses can be written as

$$\mathcal{M}_Y^{\mathrm{EGC,SS}}(\rho|\mathcal{H}_\circ) = \exp\left(\frac{\rho^2\sigma^2}{2}\right) \prod_{n=1}^{N}\int_0^{\frac{1}{2\rho}} \frac{|h_n|\exp\left(-\frac{|h_n|^2}{2\alpha_n^2}\right)}{\alpha_n^2\left(1-2\rho|h_n|\right)^u} d|h_n|, \tag{18}$$

and

$$\mathcal{M}_Y^{\mathrm{EGC,SS}}(\rho|\mathcal{H}_1) = \exp\left(\frac{\rho^2\sigma^2}{2}\right) \prod_{n=1}^{N}\int_0^{\frac{1}{2\rho}} \frac{|h_n|\exp\left(\frac{2\gamma_{\mathrm{s},n}\rho|h_n|}{1-2\rho|h_n|}\right)\exp\left(-\frac{|h_n|^2}{2\alpha_n^2}\right)}{\alpha_n^2\left(1-2\rho|h_n|\right)^u} d|h_n|, \tag{19}$$

respectively.

The above integrals can be evaluated numerically and the corresponding PDFs evaluated for the SEGC with soft sensing by making use of the relationship in (14). It is noted that the expression in (19) assumes that the $\gamma_{\mathrm{s},n}$'s are known at the FC. This assumption provides the best performance possible for the soft sensing scheme and, hence, serves as an upperbound. In the performance analysis section, we compare the performance of the soft and hard sensing and show that there are cases where hard sensing is superior to soft sensing, particularly when the SNR is sufficiently high. Before that, we address the incorporation of practical errors, such as phase errors, in the SEGC analysis.

B. Errors in Phase Estimation

We begin by analyzing the signals at the sensing nodes which are used for phase estimation.[5] Recall that the FC sends a pilot signal to all CRs so that phase information on the channels between the CRs and the FC can be acquired. Using a typical in-phase/quadrature (I/Q) receiver, the received in-phase and quadrature components at a given CR$_n$ can be written as,

$$Y_{\mathrm{I},n} = \sqrt{\gamma}|h_n|\cos\theta_n + \epsilon_{\mathrm{I},n}, \tag{20}$$

$$Y_{\mathrm{Q},n} = \sqrt{\gamma}|h_n|\sin\theta_n + \epsilon_{\mathrm{Q},n}, \tag{21}$$

where γ is the energy used by the FC to send the pilot signal, θ_n is the actual phase of the channel between the FC and CR$_n$, and where $\epsilon_{\mathrm{I},n}$ and $\epsilon_{\mathrm{Q},n}$ are the in-phase and quadrature receiver noise, each distributed according to $\mathcal{N}(0,\sigma_n^2)$.

We consider a maximum likelihood (ML) phase estimator at each CR. It can be verified in a straightforward manner that the ML estimator in this case is given by,[6]

$$\hat{\theta}_n = \tan^{-1}\left(\frac{Y_{\mathrm{Q},n}}{Y_{\mathrm{I},n}}\right). \tag{22}$$

[5]The analysis here is restricted to the hard sensing case to highlight the impact of phase errors. Extension to the soft sensing scenario is straightforward.

[6]In case more than one pilot symbol is used for phase estimation, the CR can average the in-phase and quadrature components and apply (22) to the averages. In this case, the noise variance becomes σ_n^2 divided by the number of pilot symbols.

Now, using an I/Q receiver at the FC, the received signal will be,

$$y = \sum_{n=1}^{N}|h_n|v_n\cos(\delta\theta_n) + \epsilon, \tag{23}$$

where $\delta\theta_n = \theta_n - \hat{\theta_n}$ is the difference between the true channel phase and the estimated one, pertaining to the nth CR.

Proceeding in a similar fashion to the previous section, we derive the modified MGF under the two hypotheses, now denoted $\hat{\mathcal{M}}_Y^{\mathrm{EGC,HS}}(\rho|\mathcal{H}_0)$ and $\hat{\mathcal{M}}_Y^{\mathrm{EGC,HS}}(\rho|\mathcal{H}_1)$, to be,

$$\hat{\mathcal{M}}_Y^{\mathrm{EGC,HS}}(\rho|\mathcal{H}_i) = \exp\left(\frac{1}{2}\rho^2\sigma^2\right) \prod_{n=1}^{N}\mathbb{E}\left[\exp\left(\rho|h_n|v_n\cos(\delta\theta_n)\right)|\mathcal{H}_i\right] \tag{24}$$

where $i\in\{0,1\}$. Because the MGF calculation now involves an averaging over the Bernoulli distributed v_n's, the Rayleigh random variables $|h_n|$'s and the $\delta\theta_n$'s, the expressions in (24) become quite lengthy and complicated, hence we relegate their reporting to Appendix A.

Next, we illustrate the performance of the proposed SEGC for hard sensing, soft sensing and phase errors.

IV. Performance Analysis of SEGC

In this section, we start by solving an optimization problem to derive the local and global thresholds. We then introduce a TDMA system which employs orthogonal reporting of sensing results to compare with the SEGC scheme in terms of throughput and detection performance. We also compare the performance of soft and hard sensing under the SEGC scheme and also investigate the case where MRC is employed instead of EGC. Finally, we test the robustness of the SEGC scheme against phase and synchronization errors and assess the SEGC's performance against variations in the average SNR and the reporting SNR.

A. Optimizing the Local and Global Thresholds

Here, we focus on the hard sensing scenario. Using the results of [23] and assuming Rayleigh fading for the sensing channels at all CRs, the local false-alarm and detection probabilities are given by

$$p_{\mathrm{f},n} = \Gamma_{\mathrm{inc}}(u,\lambda_n/2) \tag{25}$$

and

$$p_{\mathrm{d},n} = e^{-\frac{\lambda_n}{2}}\sum_{l=0}^{u-2}\frac{1}{l!}\left(\frac{\lambda_n}{2}\right)^l + \left(\frac{1+\overline{\gamma}_{s,n}}{\overline{\gamma}_{s,n}}\right)^{u-1}\left[e^{-\frac{\lambda_n}{2(1+\overline{\gamma}_{s,n})}} - e^{-\frac{\lambda_n}{2}}\sum_{l=0}^{u-2}\frac{1}{l!}\left(\frac{\lambda_n\overline{\gamma}_{s,n}}{2(1+\overline{\gamma}_{s,n})}\right)^l\right], \tag{26}$$

respectively, where $\Gamma_{\mathrm{inc}}(.,.)$ is the normalized incomplete Gamma function given by

$$\Gamma_{\mathrm{inc}}(x,a) = \frac{1}{\Gamma(a)}\int_0^x t^{a-1}\exp(-t)\,dt, \tag{27}$$

This article has been accepted for publication in a future issue of this journal, but has not been fully edited. Content may change prior to final publication. Citation information: DOI 10.1109/TWC.2014.2317788, IEEE Transactions on Wireless Communications

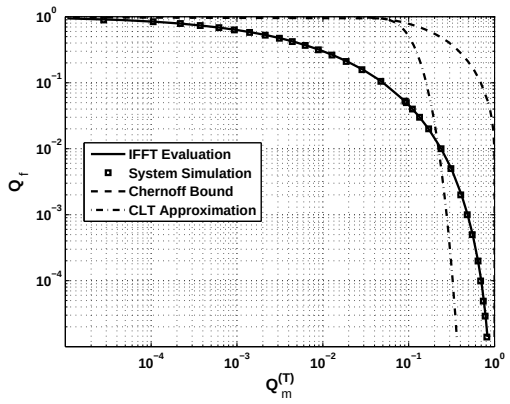

Fig. 1. Complementary receiver operation characteristics (C-ROC) curves for $N = 20$ sensors.

the quantity u is chosen to have an integer value of 5 unless otherwise stated, λ_n is the local decision threshold at CR$_n$ and $\overline{\gamma}_{s,n}$ is the average SNR of the sensing channel between the PU and CR$_n$.

In order to calculate the local and global thresholds, we consider the case when the primary network specifies a maximum miss-detection threshold, $Q_{\rm m}^{(\rm T)}$, that cannot be exceeded. The FC solves the following Neyman-Pearson-like optimization problem:

$$\begin{aligned} &\underset{\lambda,\lambda_1,\lambda_2,\ldots,\lambda_N}{\text{minimize}} \quad Q_{\rm f} \\ &\text{subject to: } Q_{\rm m} \leq Q_{\rm m}^{(\rm T)}, \end{aligned} \tag{28}$$

where λ is the global threshold at the FC as indicated in expressions (3) and (4). The problem is non-convex and can be solved numerically via gradient descent techniques for every coherence time of the channels.

Fig. 1 shows the resulting global false-alarm curve, $Q_{\rm f}$ given by (3), against the specified miss-detection probability, $Q_{\rm m}^{(\rm T)}$, for $N = 20$ sensors. The average sensing SNR is 5dB at all sensors, and the reporting SNR to the FC is also 5dB. The α_n's used in this figure are calculated to be the square root of the reporting SNR multiplied by the noise variance, i.e. $\alpha_n = \sqrt{\bar{\gamma}_{{\rm r},n}\sigma^2}$, where $\bar{\gamma}_{{\rm r},n}$ is the average reporting SNR for CR$_n$. Also shown on the figure is another curve obtained via a Monte Carlo system simulation over a large number of time slots. The results clearly validate the computation of the PDF of y from the MGF using the IFFT. Furthermore, comparing Matlab run times, we found the computational time for system simulation averages around 0.35 time units while that of the SEGC scheme averages around 0.003 time units. This means our scheme is about two orders of magnitude faster.

We also compute the Chernoff bound for the SEGC, which can be shown to be,

$$\begin{aligned} Q_{\rm f} &\leq \min_{\rho>0} \exp\left(-\rho\lambda\right) \exp\left(\frac{1}{2}\rho^2\sigma^2\right) \\ &\prod_{n=1}^{N}\left(1+\sqrt{2\pi}p_{{\rm f},n}\alpha_n\rho\exp\left(\frac{\left(\rho\alpha_n\right)^2}{2}\right)\left[1-Q(\rho\alpha_n)\right]\right), \end{aligned} \tag{29}$$

$$\begin{aligned} Q_{\rm m} &\leq \min_{\rho>0} \exp\left(\rho\lambda\right) \exp\left(\frac{1}{2}\rho^2\sigma^2\right) \\ &\prod_{n=1}^{N}\left(1-\sqrt{2\pi}p_{{\rm d},n}\alpha_n\rho\exp\left(\frac{\left(\rho\alpha_n\right)^2}{2}\right)Q(\rho\alpha_n)\right). \end{aligned} \tag{30}$$

where $Q(x) = \frac{1}{\sqrt{2\pi}}\int_x^\infty \exp\left(-\frac{t^2}{2}\right)dt$ is the tail probability of the standard normal distribution. Also superimposed on this figure, is a computation of the CLT approximation, used in [9], which can be shown to yield the following global detection probabilities,[7]

$$Q_{\rm f,CLT} = Q\left(\frac{\lambda-\mu_0}{\sigma_0}\right), \tag{31}$$

$$Q_{\rm m,CLT} = Q\left(\frac{\mu_1-\lambda}{\sigma_1}\right), \tag{32}$$

where $\mu_0 = \sqrt{\frac{\pi}{2}}\alpha N p_{\rm f}$, $\mu_1 = \sqrt{\frac{\pi}{2}}\alpha N p_{\rm d}$, $\sigma_0^2 = N\alpha p_{\rm f}\left(2-\pi p_{\rm f}/2\right)+\sigma^2$ and $\sigma_1^2 = N\alpha p_{\rm d}\left(2-\pi p_{\rm d}/2\right)+\sigma^2$. It is clear from the figure that the Chernoff bound is not tight. Also, the CLT approximation is not accurate despite the large number of sensors and the large u value.

Next, we compare the SEGC scheme with orthogonal reporting of the sensors' decisions.

B. A TDMA System and Throughput Comparison

We now consider a TDMA scheme where the FC has access to a noisy version of each sensor's decision.[8] For a fair comparison between the proposed SEGC scheme and this TDMA system, we propose the following collaborative sensing system:

1) Channel phase estimation takes place in a way that is identical to SEGC. That is, the FC sends a pilot signal to all CRs, which is used to estimate the channel phase between each CR and the FC.
2) Each CR sends its de-phased decision on a designated mini-slot within the slot duration, according to an agreed-upon schedule with the FC. This means that the received signal at the FC from CR$_n$ in the nth mini-slot will be,
$$y_n = |h_n|v_n + \epsilon_n, \tag{33}$$
where ϵ_n~$\mathcal{N}(0,\sigma^2)$.
3) The FC now makes its global decision by calculating the following log-likelihood ratio (LLR),
$$\text{LLR}_{\rm TDMA} = \sum_{n=1}^{N}\frac{f(y_n|\mathcal{H}_0)}{f(y_n|\mathcal{H}_1)} \underset{\mathcal{H}_1}{\overset{\mathcal{H}_0}{\gtrless}} \lambda, \tag{34}$$
where the PDFs $f(y_n|\mathcal{H}_0)$ and $f(y_n|\mathcal{H}_1)$ can be attained in closed-form (cf. Appendix B). The global false-alarm and miss-detection probabilities are given by $\Pr\{\text{LLR}_{\rm TDMA} < \lambda|\mathcal{H}_0\}$ and $\Pr\{\text{LLR}_{\rm TDMA} > \lambda|\mathcal{H}_1\}$, respectively. Note that this use of the LLR is the optimal

[7]For simplicity, here we assume identical local detection probabilities at the cognitive nodes so that $p_{{\rm f},n} = p_{\rm f}$ and $p_{{\rm d},n} = p_{\rm d}$. We also assume identical reporting channels so that $\alpha_n = \alpha$.

[8]The analysis is carried out here for the hard sensing case. Extension to the soft sensing case is straightforward.

This article has been accepted for publication in a future issue of this journal, but has not been fully edited. Content may change prior to final publication. Citation information: DOI 10.1109/TWC.2014.2317788, IEEE Transactions on Wireless Communications

fusion of the various observations. Various suboptimal approaches exist such as, for instance, decoding each binary decision v_n using y_n and then fusing the decoded decisions using the OR, AND, or K-out-of-N rules. Our choice here gives the best possible performance for the TDMA system.

In addition to computing the detection error probabilities, we also use throughput as a performance metric that is more relevant in the context of CR. It is possible under a TDMA scheme to wait for a large number of observations and reduce the detection errors to very small values. Nevertheless, the PU may change its state of activity over a relatively short period, thereby making it necessary for the CR to make a fast, yet reliable, decision in order to obtain a transmission opportunity. This requirement creates a sensing reliability-throughput tradeoff that is characteristic of CR operation [10].

Under the SEGC scheme, we define throughput as

$$R_{\rm SEGC} = (1 - Q_{\rm f}) \left(\frac{T - \tau - \tau_s}{T} \right) r_s, \qquad (35)$$

where $Q_{\rm f}$ is given by (3), T is the time slot duration, τ is the time taken by the CRs to send their sensing decisions to the FC, τ_s is the fraction of time used by the CRs to carry out local sensing and r_s is the mean transmission rate achieved by the secondary node that seizes the transmission opportunity.[9] In the above, we assume that miss-detection leads to the loss of the secondary packet and, hence, no rate is achieved.

For the TDMA scheme, on the other hand, we have

$$R_{\rm TDMA} = (1 - Q_{\rm f,TDMA}) \left(\frac{T - N\tau - \tau_s}{T} \right)^+ r_s, \qquad (36)$$

where $(x)^+ = \max\{x, 0\}$ and $Q_{\rm f,TDMA}$ is the global false alarm probability for the TDMA scheme, calculated numerically as the $\Pr\{\text{LLR}_{\rm TDMA} < \lambda | \mathcal{H}_0\}$. Note that, as expected, the throughput of the TDMA scheme could drop to zero as the number of sensors, N, increases.

Given the above equations, our throughput-based optimization problem is formulated as follows

$$\begin{aligned} &\underset{\lambda, \lambda_1, \lambda_2, \ldots, \lambda_N}{\text{maximize}} \quad R \\ &\text{subject to: } Q_{\rm m} \leq Q_{\rm m}^{(\rm T)}, \end{aligned} \qquad (37)$$

where R is the throughput given by (35) and (36) for the SEGC and TDMA schemes, respectively.

Fig. 2 shows the solution of the problem (28) for the SEGC scheme and the outlined TDMA system for the case of $N = 30$ sensors. The average sensing SNR is set to the same value for both schemes (5dB) so that we can evaluate the difference in their performances over the sensor reporting part only. The PDF of the $\text{LLR}_{\rm TDMA}$ is computed numerically using y_n's generated from the PDFs $f(y_n|\mathcal{H}_0)$ and $f(y_n|\mathcal{H}_1)$. As observed, the performance of both systems degrades with the decrease in reporting SNR value. The degradation is negligible in the case of SEGC, which shows the robustness of the system towards variations in the reporting SNR. The performance of the TDMA system, however, varies dramatically with the reporting SNR. In the low-SNR regime, where each TDMA reading suffers from noise albeit being decoded separately, SEGC is superior. The TDMA scheme does not improve significantly above the SEGC except in the high-SNR case.

[9]We assume here that once a vacancy is observed, one CR seizes the transmission opportunity.

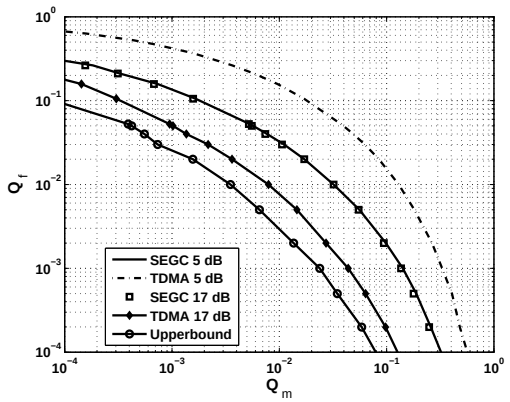

Fig. 2. C-ROC curves for $N = 30$ sensors for the SEGC and TDMA schemes at reporting SNRs of 5dB and 17dB.

Also superimposed on the curve is the resulting ROC for an upperbound system which we construct through the use of [16]. In that work, orthogonal reporting of sensors' decisions is employed. However, the reporting is perfect, i.e. no channel fading or AWGN exists. It is not difficult to see in this case why the resulting ROC upperbounds the proposed SEGC scheme. To setup the comparison, we use the same $\text{LLR}_{\rm TDMA}$ metric as in (34). However, in this case the PDFs $f(y_n|\mathcal{H}_0)$ and $f(y_n|\mathcal{H}_1)$ are readily attainable as

$$f(y_n|\mathcal{H}_0) = p_{{\rm f},n}^{v_n} \left(1 - p_{{\rm f},n}\right)^{1 - v_n}, \qquad (38)$$

$$f(y_n|\mathcal{H}_1) = p_{{\rm d},n}^{v_n} \left(1 - p_{{\rm d},n}\right)^{1 - v_n}. \qquad (39)$$

It is noted that the gap is wide between the proposed solution and the upperbound. However, Fig. 3 shows the achievable throughput by solving (37) for the SEGC and the TDMA schemes, in addition to the upperbound system. The superiority of the SEGC scheme to the upperbound and the other TDMA schemes is clear and is mainly because of the short reporting overhead. Things improve a bit for the TDMA system with the increase in the reporting SNR. However, the achievable throughput remains far from what is possible using the SEGC. For this figure, we chose $\tau = 0.01T$ while $\tau_s = 0.005T$.[10]

Having compared the SEGC with orthogonal reporting techniques, we now proceed to making a comparison with another technique which also uses simultaneous transmission of sensors' decisions.

C. Comparing MRC and SEGC under the Hard and Soft Sensing Scenarios

Herein, we investigate whether the cooperative sensing performance can be improved over SEGC by making available

[10]The value of τ is selected to be of the same order of magnitude as the suggested values in [24], while τ_s is set to a reasonable value given the sensing SNR of 5dB and the sensing-throughput tradeoff as highlighted in [10].

This article has been accepted for publication in a future issue of this journal, but has not been fully edited. Content may change prior to final publication. Citation information: DOI 10.1109/TWC.2014.2317788, IEEE Transactions on Wireless Communications

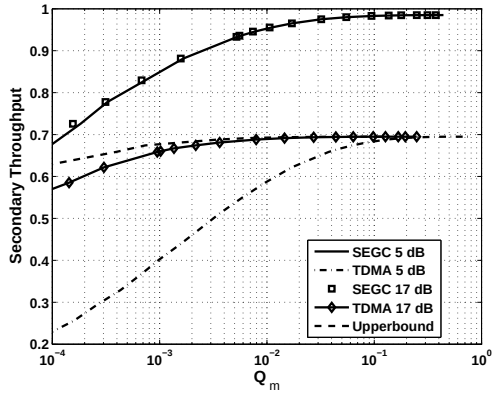

Fig. 3. Throughput of the SEGC and the TDMA schemes at reporting SNRs of 5dB and 17dB.

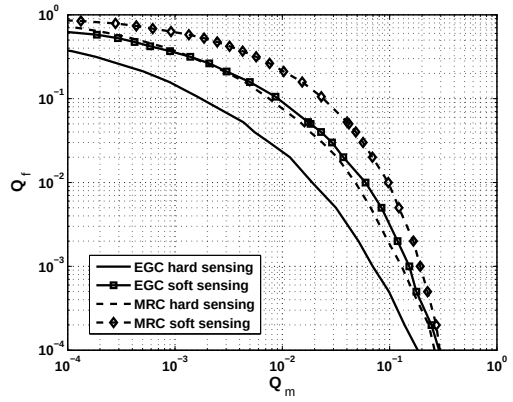

Fig. 4. Comparison between SEGC and MRC of sensors' decisions for $N = 10$ sensors under both soft-sensing and hard-sensing. The sensing SNR is set to 10dB, the reporting SNR is -10dB and $u = 1$. SEGC with hard-sensing gives the best performance.

both channel phase and magnitude at each CR, in analogy to the gains achieved by wireless communication diversity techniques employing MRC, which requires knowledge of channel gain and magnitude.

When MRC is used, the FC's received signal is given by,

$$y = \sum_{n=1}^{N} \frac{|h_n|^2}{\sqrt{2\alpha_n^2}} v_n + \epsilon, \tag{40}$$

i.e. the weight factor is $w_n = h_n/\sqrt{2\alpha_n^2}$. Based on (1), we note that the average transmit power of each local sensor will be $\mathbb{E}(|w_n|^2 v_n^2) = \mathbb{E}(|w_n|^2)\mathbb{E}(v_n^2)$. The normalization by the channel's α_n value in (40) above ensures that MRC will have the same *average* transmit power as the corresponding SEGC, for fair comparison.

By doing a similar analysis to the SEGC scheme and noting that now the $|h_n|^2$'s are exponentially distributed random variables with parameter α_n, we may write the MGF of the MRC scheme as follows

$$\mathcal{M}_Y^{\mathrm{MRC,HS}}(\rho|\mathcal{H}_\circ) = \exp\left(\frac{1}{2}\rho^2\sigma^2\right) \prod_{n=1}^{N}\left(1 - p_{\mathrm{f},n} + p_{\mathrm{f},n}\left(1 - \frac{\alpha_n\rho}{\sqrt{2}}\right)^{-1}\right), \tag{41}$$

$$\mathcal{M}_Y^{\mathrm{MRC,HS}}(\rho|\mathcal{H}_1) = \exp\left(\frac{1}{2}\rho^2\sigma^2\right) \prod_{n=1}^{N}\left(1 - p_{\mathrm{d},n} + p_{\mathrm{d},n}\left(1 - \frac{\alpha_n\rho}{\sqrt{2}}\right)^{-1}\right). \tag{42}$$

We can then derive the PDFs using the IFFT method, as was previously done throughout the paper.

Interestingly enough, we find that SEGC does perform better than MRC in many cases. Figures 4 and 5 show the achievable C-ROC, i.e. Q_{f} versus Q_{m} curve, of the proposed SEGC in comparison to the MRC scheme for both hard and soft sensing under variation of the different system parameters. Specifically, we highlight cases where hard sensing is better than soft sensing and where soft sensing is better than hard

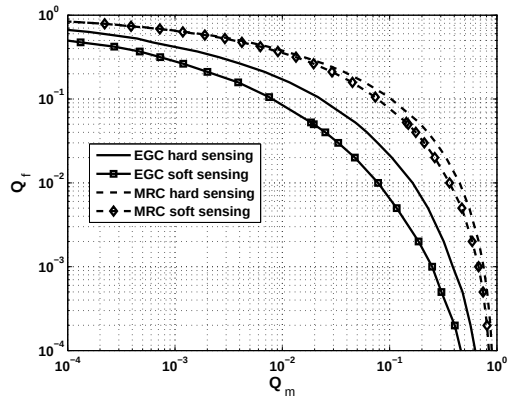

Fig. 5. Comparison between SEGC and MRC of sensors' decisions for $N = 40$ sensors under both soft-sensing and hard-sensing. The sensing and reporting SNRs are set to 0dB and $u = 1$. SEGC with soft sensing provides the best performance.

sensing. In both cases, the SEGC scheme is superior to the MRC one. Previous work, e.g. [11], [12], also report cases where EGC is better than MRC, in an orthogonal reporting setting. In Appendix C, we provide a more detailed discussion on this topic.

D. Impact of Phase and Synchronization Errors on SEGC Performance

Figure 6 shows the achievable performance under the consideration of errors in the phase estimate. Also imposed on this figure is the system simulation results with phase errors. The loss in performance is small and improves by increasing the value of γ, which is the energy of the pilot symbol transmitted by the FC.

In Fig. 7, we plot the SEGC performance when both synchronization and phase errors occur. To calculate the synchronization error, we consider the transmission of rectangular pulses of duration τ by each CR. This means that the received

This article has been accepted for publication in a future issue of this journal, but has not been fully edited. Content may change prior to final publication. Citation information: DOI 10.1109/TWC.2014.2317788, IEEE Transactions on Wireless Communications

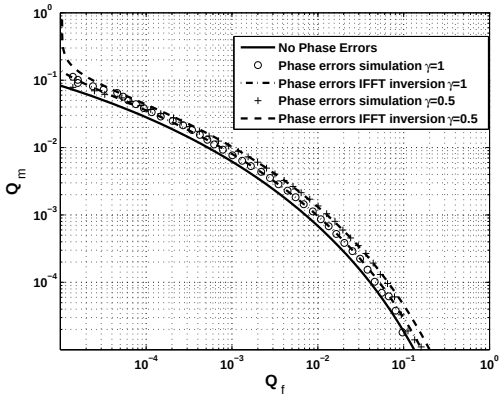

Fig. 6. SEGC performance under phase errors, which cause an increase in Q_{m}. The degradation is reduced by increasing the energy of pilot symbols, γ. Also shown are curves obtained via system simulation for validation purposes.

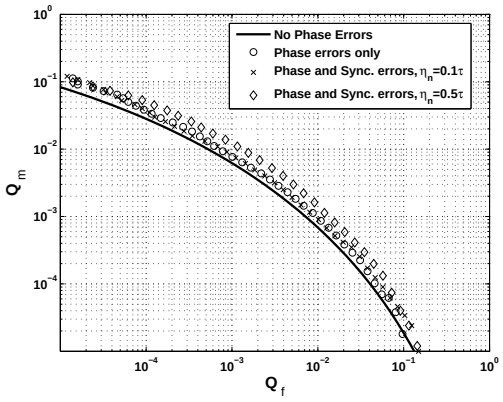

Fig. 7. SEGC performance under phase and synchronization errors for $\gamma = 1$.

signal now is,

$$y = \sum_{n=1}^{N} |h_n| v_n \cos(\delta\theta_n) \left(1 - \frac{|\eta_n|}{\tau}\right) + \epsilon, \qquad (43)$$

where τ is the time interval during which the sensors transmit their decisions to the FC and η_n is the timing error between CR_n and the FC. The reported results are for uniformly distributed η_n's from $[-0.1\tau, 0.1\tau]$ and also for the case of η_n's uniformly distributed in $[-0.5\tau, 0.5\tau]$. The results clearly demonstrate the robustness of SEGC to synchronization errors, which can be explained by the fact that such errors lead to reduction in the effective SNR at the FC. SEGC, however, is robust to variations in the reporting SNR as demonstrated by Fig. 8 which shows the variation of the minimum Q_{f} with the SNR, for both the sensing SNR and the reporting SNR. It is clear that performance improves significantly when the sensing SNR improves. On the other hand, fluctuations in the reporting SNR have a relatively weak impact on performance, further validating the robustness of our SEGC scheme to variations in the reporting SNR.

V. Conclusion

We proposed a collaborative sensing scheme for cognitive radio networks termed sensing with equal gain combining

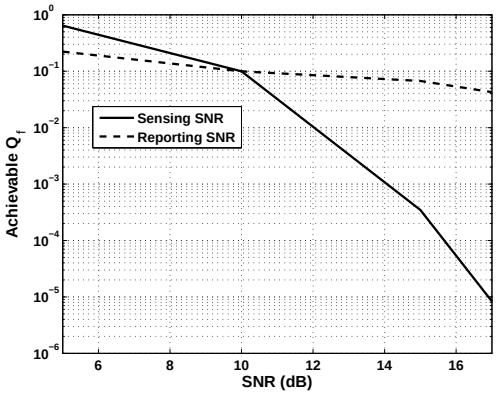

Fig. 8. Variation of the minimum Q_{f} with the SNR.

(SEGC). Under the SEGC scheme, sensor nodes simultaneously transmit their sensing decisions to be coherently combined at the fusion center. We obtained the global detections probabilities exactly through an MGF approach. We considered both cases of hard and soft sensing and provided communication scenarios where hard sensing is superior to its soft counterpart. Contrary to the schemes implementing orthogonal reporting of sensors' decisions, our findings document instances where hard sensing is superior to soft sensing. We also compared our approach with the MRC scheme and showed examples where the SEGC method, bearing only the cost of channel phase information, is superior. From the reliability of detection perspective, the proposed approach outperforms a comparison TDMA system at low SNRs. From a secondary throughput perspective, our scheme always outperforms TDMA and other orthogonal decision reporting techniques where throughput suffers with the increase in the number of sensors. We also characterized our system performance from the perspective of variation of the sensing and reporting SNRs and with consideration to phase and synchronization errors as encountered in practice. We showed the robustness of our scheme under such circumstances.

Appendix A
Evaluation of MGFs under Errors in Phase Estimation

To calculate (24), we need to evaluate the term $\mathbb{E}\left(\exp\left(\rho|h_n|v_n\cos(\delta\theta_n)\right)|\mathcal{H}_i\right)$, $i \in \{0,1\}$, for every sensing node n. Herein, we drop the index dependency for notational convenience and define $g = |h|$. We also drop the conditioning on the hypotheses. Thus, we may write,

$$\mathbb{E}\left(\exp\left(\rho g v\,\cos(\delta\theta)\right)\right) = \sum_{v=0,1} \int_0^{2\pi} \int_0^{\infty} \exp(\rho v g\, cos(\delta\theta)) f(\delta\theta|g) f(g) dg d\delta\theta p(v). \qquad (44)$$

Then averaging over the decisions v, we get

$$\mathbb{E}\left(\exp\left(\rho g v\,\cos(\delta\theta)\right)\right) = p(v=0) + p(v=1) \int_0^{2\pi} \int_0^{\infty} \exp(\rho g\, cos(\delta\theta)) f(\delta\theta|g) f(g) dg d\delta\theta. \qquad (45)$$

This article has been accepted for publication in a future issue of this journal, but has not been fully edited. Content may change prior to final publication. Citation information: DOI 10.1109/TWC.2014.2317788, IEEE Transactions on Wireless Communications

where $p(v=0)$ is obtained as,

$$p(v=0)=\begin{cases}1-p_{\rm f} & \text{under } \mathcal{H}_0\\ 1-p_{\rm d} & \text{under } \mathcal{H}_1,\end{cases} \tag{46}$$

while $p(v=1)$ is calculated as,

$$p(v=1)=\begin{cases}p_{\rm f} & \text{under } \mathcal{H}_0\\ p_{\rm d} & \text{under } \mathcal{H}_1.\end{cases} \tag{47}$$

To evaluate (45), we need to derive the PDF of the estimated phase error, conditioned on a particular channel realization, $f(\delta\theta|g)$. Using (20) and (21), define an auxiliary random variable Z such that

$$Z=\sqrt{Y_{\rm I}^2+Y_{\rm Q}^2}. \tag{48}$$

By a simple transformation of random variables from Y_I and Y_Q to Z and $\delta\theta$, the joint PDF of Z and $\delta\theta$, $f(Z,\delta\theta|g)$, may be attained as

$$f(Z,\delta\theta\big|g)=\frac{Z}{2\pi\sigma^2}\exp\left(-\frac{Z^2+\gamma g^2-2Z\sqrt{\gamma}g\cos(\delta\theta)}{2\sigma^2}\right). \tag{49}$$

Integrating over Z, we get

$$f\left(\delta\theta|g\right)=\frac{1}{2\pi}\exp\left(-\eta g^2\right)+\sqrt{\frac{\eta}{\pi}}g\cos\left(\delta\theta\right)\exp\left(-\eta g^2+\eta g^2\cos^2\left(\delta\theta\right)\right)$$
$$-\sqrt{\frac{\eta}{\pi}}g\cos\left(\delta\theta\right)\exp\left(-\eta g^2\right)\exp\left(\eta g^2\cos^2\left(\delta\theta\right)\right)Q\left(\cos\left(\delta\theta\right)\sqrt{2\gamma g^2}\right), \tag{50}$$

where $\eta=\frac{\gamma}{2\sigma^2}$. Next, we evaluate the integral $\int_0^\infty \exp(\rho g\, cos(\delta\theta))f(\delta\theta|g)f(g)dg$ in (45). From (50), there are three expressions to evaluate and we take each separately. For the first expression, we have

$$\int_0^\infty \exp\left(-\eta g^2\right)\exp\left(\rho g\cos\left(\delta\theta\right)\right)\frac{g}{2\pi\alpha^2}\exp\left(-\frac{g}{2\alpha^2}\right)dg=$$
$$\exp\left(\frac{\rho^2\cos^2\left(\delta\theta\right)}{4w}\right)$$
$$\int_{\frac{\rho^2\cos^2(\delta\theta)}{4w}}^\infty \exp\left(-\beta\right)\left[\frac{\rho\cos\left(\delta\theta\right)}{2w}+\frac{\beta^{1/2}}{\sqrt{w}}\right]\frac{d\beta}{2\pi\alpha^2 2\sqrt{\beta w}}, \tag{51}$$

where $\beta=\left[g-\frac{\rho\cos(\delta\theta)}{2w}\right]^2$, $w=\eta+\frac{1}{2\alpha^2}$ and we arrive at the equation above by a change of integration variables. Continuing further, we get

$$\exp\left(\frac{\rho^2\cos^2\left(\delta\theta\right)}{4w}\right)\int_{\frac{\rho^2\cos^2(\delta\theta)}{4w}}^\infty\exp\left(-\beta\right)\left[\frac{\rho\cos\left(\delta\theta\right)}{4w^{3/2}}\beta^{-\frac{1}{2}}+\frac{1}{2w}\right]\frac{d\beta}{2\pi\alpha^2}=$$
$$\frac{1}{4\pi w\alpha^2}+\frac{\rho\cos\left(\delta\theta\right)\exp\left(\frac{\rho\cos^2(\delta\theta)}{4w}\right)}{8\sqrt{\pi}\alpha^2w^{3/2}}\left[1-\Gamma_{\rm inc}\left(\frac{\rho^2\cos^2\left(\delta\theta\right)}{4w},\frac{1}{2}\right)\right]. \tag{52}$$

Proceeding in the same fashion for the second expression, we obtain (53), on the next page, where $x=\eta\sin^2\left(\delta\theta\right)+\frac{1}{2\alpha^2}$. The third expression, given by

$$-\sqrt{\frac{\eta}{\pi}}\frac{\cos\left(\delta\theta\right)}{2\pi\alpha^2}\int_0^\infty g^2\exp\left(-g^2x+\rho g\cos\left(\delta\theta\right)\right)Q\left(\sqrt{2\gamma}g\cos\left(\delta\theta\right)\right)dg, \tag{54}$$

is evaluated numerically using Matlab. Finally, all the attained terms, (52), (53) and (54), need to be averaged out with respect to $\delta\theta$, which we also implement in Matlab. Having obtained the MGFs, we can proceed to obtain the PDFs via the IFFT procedure and then compute the detection error probabilities.

Appendix B
The PDFs under the TDMA Scheme

Using equation (33), we write

$$f\left(y_n|h_n,\mathcal{H}_\circ\right)=\frac{1-p_{{\rm f},n}}{\sqrt{2\pi}\sigma}\exp\left(-\frac{y_n^2}{2\sigma^2}\right)+\frac{p_{{\rm f},n}}{\sqrt{2\pi}\sigma}\exp\left(-\frac{\left(y_n-|h_n|\right)^2}{2\sigma^2}\right), \tag{55}$$

and similarly,

$$f\left(y_n|h_n,\mathcal{H}_1\right)=\frac{1-p_{{\rm d},n}}{\sqrt{2\pi}\sigma}\exp\left(-\frac{y_n^2}{2\sigma^2}\right)+\frac{p_{{\rm d},n}}{\sqrt{2\pi}\sigma}\exp\left(-\frac{\left(y_n-|h_n|\right)^2}{2\sigma^2}\right). \tag{56}$$

By averaging out the channel gains, we arrive at

$$f\left(y_n|\mathcal{H}_\circ\right)=\frac{1-p_{{\rm f},n}}{\sqrt{2\pi}\sigma}\exp\left(-\frac{y_n^2}{2\sigma^2}\right)+\frac{p_{{\rm f},n}}{\sqrt{2\pi}\sigma}A \tag{57}$$

and

$$f\left(y_n|\mathcal{H}_1\right)=\frac{1-p_{{\rm d},n}}{\sqrt{2\pi}\sigma}\exp\left(-\frac{y_n^2}{2\sigma^2}\right)+\frac{p_{{\rm d},n}}{\sqrt{2\pi}\sigma}A, \tag{58}$$

respectively, where A can be evaluated to be

$$A=\frac{1}{2\zeta_n}\exp\left(-\frac{y_n^2}{4\sigma^4\zeta_n}\right)+\sqrt{\frac{\pi}{\zeta_n}}\left(\frac{y_n}{2\sigma^2\zeta_n}\right)\exp\left(-\frac{y_n^2\zeta_n}{\alpha_n^2}\right)\left(1-Q\left(\frac{y_n}{\sigma^2\sqrt{2\zeta_n}}\right)\right), \tag{59}$$

with $\zeta_n=\frac{1}{2}\left(\frac{1}{\alpha_n^2}+\frac{1}{\sigma^2}\right)$.

Appendix C
MRC versus EGC of Sensors' Decisions

In this appendix, we briefly discuss the selection of the weights w_n in (1). In a transmit diversity context, with known channel state information, the received signal is

$$y=\sum_{n=1}^N w_n^*h_ns+\epsilon,$$

where symbol s is transmitted from all the antennas. In that case, it can be shown that $w_n\propto h_n$, i.e. MRC, maximizes the received SNR and, hence, is optimal in this setting [25]. On the other hand, in the distributed detection scenario considered in this paper, possibly different symbols are transmitted by the different sensors and a question arises as to what could be the optimal weighting vector if we extend the optimization problem in (28) to include the weights. This extension would significantly increase the complexity of the problem. So, in order to gain insight into the proper choice of w_n and to explain our results which show that MRC is not necessarily optimal in a distributed detection setting, we consider a simpler optimization problem that instead considers the deflection coefficient as an objective.

This article has been accepted for publication in a future issue of this journal, but has not been fully edited. Content may change prior to final publication. Citation information: DOI 10.1109/TWC.2014.2317788, IEEE Transactions on Wireless Communications

$$\frac{\sqrt{\eta}\cos(\delta\theta)}{2\pi^{3/2}\alpha^2}\int_0^\infty g^2\exp\left(-\eta g^2\right)\exp\left(\eta g^2\cos^2(\delta\theta)\right)\exp\left(-\frac{g^2}{2\alpha^2}\right)\exp\left(\rho g\cos(\delta\theta)\right)dg=\frac{\sqrt{\eta}\cos(\delta\theta)}{4\pi^{3/2}\alpha^2\sqrt{x}}\left[\frac{\rho\cos(\delta\theta)}{x^{3/2}}\right.$$
$$\left.+\exp\left(\frac{\rho^2\cos^2(\delta\theta)}{4x}\right)\frac{\rho^2\cos^2(\delta\theta)\sqrt{\pi}}{4x^2}\left(1-\Gamma_{\rm inc}\left(\frac{\rho^2\cos^2(\delta\theta)}{4x},1/2\right)\right)+\exp\left(\frac{\rho^2\cos^2(\delta\theta)}{4x}\right)\frac{\sqrt{\pi}}{2x}\left(1-\Gamma_{\rm inc}\left(\frac{\rho^2\cos^2(\delta\theta)}{4x},3/2\right)\right)\right], \tag{53}$$

Specifically, we aim to maximize the modified deflection coefficient (MDC) [26], given by

$$d^2=\frac{|\mathbb{E}(y|\mathcal{H}_1)-\mathbb{E}(y|\mathcal{H}_0)|^2}{\mathrm{var}(y|\mathcal{H}_1)}, \tag{60}$$

where var denotes the variance of a random variable. Given (1), it can be easily shown that

$$\mathbb{E}(y|\mathcal{H}_0)=\sum_{n=1}^{N}w_n^*h_np_{\mathrm{f},n}, \tag{61}$$

$$\mathbb{E}(y|\mathcal{H}_1)=\sum_{n=1}^{N}w_n^*h_np_{\mathrm{d},n} \tag{62}$$

and

$$\mathrm{var}(y|\mathcal{H}_1)=\sigma^2+\sum_{n=1}^{N}|w_n|^2|h_n|^2p_{\mathrm{d},n}\left(1-p_{\mathrm{d},n}\right). \tag{63}$$

Note that

$$\mathbb{E}(y|\mathcal{H}_1)-\mathbb{E}(y|\mathcal{H}_0)=\mathbf{w}^*\mathbf{g}, \tag{64}$$

where $\mathbf{g}=\left[h_1\left(p_{\mathrm{d},1}-p_{\mathrm{f},1}\right)...h_N\left(p_{\mathrm{d},N}-p_{\mathrm{f},N}\right)\right]^{\mathrm{T}}$, $\mathbf{w}=[w_1,w_2,...w_N]$ is the vector of sensor weights and $(.)^{\mathrm{T}}$ denotes the transpose operation.[11] Defining $\mathbf{m}=\left[|h_1|^2p_{\mathrm{d},1}\left(1-p_{\mathrm{d},1}\right)...|h_N|^2p_{\mathrm{d},N}\left(1-p_{\mathrm{d},N}\right)\right]^{\mathrm{T}}$ and $\mathbf{M}$ as the $N\times N$ diagonal matrix with the elements of $\mathbf{m}$ on the main diagonal, then the MDC as defined in (60) can be equivalently written as

$$d^2=\frac{|\mathbf{w}^*\mathbf{g}|^2}{\sigma^2+\mathbf{w}^*\mathbf{M}\mathbf{w}}. \tag{65}$$

Applying the Cauchy-Schwarz inequality, it can then be shown that d^2 is maximized by choosing the weights according to:

$$w_n\propto\frac{h_n\left[p_{\mathrm{d},n}-p_{\mathrm{f},n}\right]}{\sigma^2+|h_n|^2p_{\mathrm{d},n}\left[1-p_{\mathrm{d},n}\right]}, \tag{66}$$

which is clearly *not* the MRC result.

Note that the discussion above is only an attempt to refute, analytically, the idea that MRC is always optimal, regardless of the specific communication setting. We maintain that the above-obtained weights are for maximizing the MDC. In future extension of this work, we attempt to solve for the optimal weights and thresholds of problems (28) and (37).

In Fig. 9, we plot the resulting Q_m curve with respect to variations in the reporting SNR for the EGC, MRC, and the deflection coefficient based combining (DCC) schemes. For this curve, $Q_f=0.05$, while the sensing SNR is fixed at 5dB. The figure demonstrates that the optimal weight vector for the problem of (28) remains different from the DCC and the EGC solutions. However, the suggested SEGC does perform better than the DCC for a large range of the reporting SNR. The MRC, on the other hand, is nowhere to be optimal in that figure. Because of the simplicity of its solution and ease of implementation, we chose to use the EGC method.

[11]We use lower-case boldface letters to denote vectors and upper-case boldface letters to denote matrices.

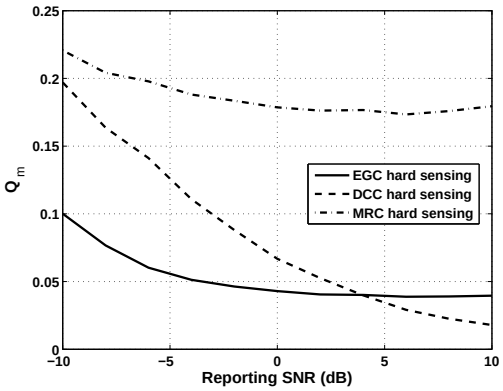

Fig. 9. Variation of the minimum Q_{m} with the reporting SNR for the SEGC, MRC and the DCC weights using 20 sensors.

ACKNOWLEDGMENT

The authors wish to thank Mohamed-Slim Alouini and Amal Hyadi for technical discussions on this work.

REFERENCES

[1] A. Ghasemi and E. Sousa, "Collaborative spectrum sensing for opportunistic access in fading environments," in *Proc. IEEE Dynamic Spectrum Access Networks (DySPAN)*, Baltimore, MD, 2005, pp. 131–136.

[2] S. M. Mishra, A. Sahai, and R. W. Brodersen, "Cooperative Sensing Among Cognitive Radios," in *Proc. IEEE Int. Conf. Commun. (ICC)*, Istanbul, Turkey, 2006, pp. 1658–1663.

[3] Z. Quan, S. Cui, H. V. Poor, and A. H. Sayed, "Collaborative wideband sensing for cognitive radios," *IEEE Signal Process. Mag.*, vol. 25, no. 6, pp. 60–73, Nov. 2008.

[4] S. Zahabi, A. Tadaion, and S. Aissa, "Neyman-pearson cooperative spectrum sensing for cognitive radio networks with fine quantization at local sensors," *IEEE Trans. Commun.*, vol. 60, no. 6, pp. 1511–1522, June 2012.

[5] J. Yang and S. Ulukus, "Delay-minimal transmission for average power constrained multi-access communications," *IEEE Trans. Wireless Commun.*, vol. 9, no. 9, pp. 2754–2767, Sep. 2010.

[6] A. Anandkumar and L. Tong, "Type-based random access for distributed detection over multiaccess fading channels," *IEEE Trans. Signal Process.*, vol. 55, no. 10, pp. 5032–5043, Oct. 2007.

[7] F. Li, J. Evans, and S. Dey, "Decision fusion over noncoherent fading multiaccess channels," *IEEE Trans. Signal Process.*, vol. 59, no. 9, pp. 4367–4380, Sep. 2011.

[8] C. Berger, M. Guerriero, S. Zhou, and P. Willett, "PAC vs. MAC for decentralized detection using noncoherent modulation," *IEEE Trans. Signal Process.*, vol. 57, no. 9, pp. 3562–3575, Sep. 2009.

[9] S. Zhang, T. Wu, and V. Lau, "A low-overhead energy detection based cooperative sensing protocol for cognitive radio systems," *IEEE Trans. Wireless Commun.*, vol. 8, no. 12, pp. 5761–5766, Dec. 2009.

This article has been accepted for publication in a future issue of this journal, but has not been fully edited. Content may change prior to final publication. Citation information: DOI 10.1109/TWC.2014.2317788, IEEE Transactions on Wireless Communications

[10] Y.-C. Liang, Y. Zeng, E. C. Y. Peh, and A. T. Hoang, "Sensing-throughput tradeoff for cognitive radio networks," *IEEE Trans. Wireless Commun.*, vol. 7, no. 4, pp. 1326–1337, Apr. 2008.

[11] R. Niu, B. Chen, and P. K. Varshney, "Decision fusion rules in wireless sensor networks using fading channel statistics," in *Conf. Inform. Sci. and Syst.*, Baltimore, MD, Mar. 2003.

[12] V. Kanchumarthy, R. Viswanathan, and M. Madishetty, "Impact of channel errors on decentralized detection performance of wireless sensor networks: A study of binary modulations, rayleigh-fading and nonfading channels, and fusion-combiners," *IEEE Trans. Signal Process.*, vol. 56, no. 5, pp. 1761–1769, May 2008.

[13] J. G. Proakis and M. Salehi, *Digital Communications*, 5th ed. New York: McGraw-Hill, Nov. 2007.

[14] A. El-Saleh, M. Ismail, M. Akbari, M. Manesh, and S. Zavareh, "Minimizing the detection error of cognitive radio networks using particle swarm optimization," in *Proc. Int. Conf. Comput. Commun. Eng. (ICCCE)*, Kuala Lumpur, Malaysia, July 2012, pp. 877–881.

[15] T. Nguyen, V. Abdul Rahim, K. Le, H. Nguyen, and P. Nguyen, "Numerical comparisons of cooperative spectrum sensing algorithms over rayleigh fading channel," in *2013 Annu. Int. Conf. Emerging Research Areas and Int. Conf. on Microelectron., Commun. Renewable Energy (AICERA/ICMiCR)*, Kanjirappally, India, June 2013, pp. 1–6.

[16] J. Ma, G. Zhao, and Y. Li, "Soft combination and detection for cooperative spectrum sensing in cognitive radio networks," *IEEE Trans Wireless Commun.*, vol. 7, no. 11, pp. 4502–4507, Nov. 2008.

[17] S. Chaudhari, J. Lunden, V. Koivunen, and H. Poor, "Cooperative sensing with imperfect reporting channels: Hard decisions or soft decisions?" *IEEE Trans. Signal Process*, vol. 60, no. 1, pp. 18–28, Jan. 2012.

[18] F. Suratman, A. Tetz, and A. Zoubir, "Collaborative spectrum sensing using sequential detections: Soft decision vs. hard decision," in *Int. Conf. Inform. and Commun. Technol. (ICoICT)*, Bandung, Indonesia, 2013, pp. 1–6.

[19] J. Hillenbrand, T. Weiss, and F. Jondral, "Calculation of detection and false alarm probabilities in spectrum pooling systems," *IEEE Commun. Lett.*, vol. 9, no. 4, pp. 349–351, Apr. 2005.

[20] L. A. Waller, B. W. Turnbull, and J. M. Hardin, "Obtaining distribution functions by numerical inversion of characteristic functions with applications," *Amer. Stat.*, vol. 49, no. 4, pp. 346–350, Nov. 1995.

[21] P. Hughett, "Error bounds for numerical inversion of a probability characteristic function," *SIAM J. Numerical Anal.*, vol. 35, no. 4, pp. 1368–1392, Aug. 1998.

[22] M. Abramowitz and I. Stegun, *Handbook of Mathematical Functions with Formulas, Graphs, and Mathematical Tables*. New York: Dover Publications, 1972.

[23] F. Digham, M. Alouini, and M. Simon, "On the energy detection of unknown signals over fading channels," *IEEE Trans. Commun.*, vol. 55, no. 1, pp. 21–24, Jan. 2007.

[24] C. Wang, "Cooperation strategies for secondary users," QUASAR Deliverable D4.2, Tech. Rep., Mar 31, 2012.

[25] J. R. Barry, E. A. Lee, and D. G. Messerschmitt, *Digital Communication*, 3rd ed. Springer, 2004.

[26] Z. Quan, S. Cui, and A. Sayed, "Optimal linear cooperation for spectrum sensing in cognitive radio networks," *IEEE J. Sel. Topics Signal Process.*, vol. 2, no. 1, pp. 28–40, Feb. 2008.

Doha Hamza (S'12) received the B.S. degree in electrical engineering from Alexandria University, Egypt, and the M.S. degree in wireless communications from Nile University, Egypt. She is currently a PhD candidate at King Abdullah University of Science and Technology (KAUST), working on cross-layer design of cognitive radio networks.

Her current research interests are dynamic spectrum access, cognitive radio networks, game-theory application to wireless communications, and cross-layer design.

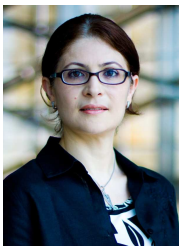

Sonia Aïssa (S'93-M'00-SM'03) received her Ph.D. degree in Electrical and Computer Engineering from McGill University, Montreal, QC, Canada, in 1998. Since then, she has been with the Institut National de la Recherche Scientifique-*Energy, Materials and Telecommunications* Center (INRS-EMT), University of Quebec, Montreal, QC, Canada, where she is a Professor of Telecommunications.

From 1996 to 1997, she was a Researcher with the Department of Electronics and Communications of Kyoto University, and with the Wireless Systems Laboratories of NTT, Japan. From 1998 to 2000, she was a Research Associate at INRS-EMT, Montreal. In 2000-2002, while she was an Assistant Professor, she was a Principal Investigator in the major program of personal and mobile communications of the Canadian Institute for

Telecommunications Research, leading research in radio resource management for wireless networks. From 2004 to 2007, she was an Adjunct Professor with Concordia University, Montreal. In 2006, she was Visiting Invited Professor with the Graduate School of Informatics, Kyoto University, Japan. Her research interests lie in the area of wireless and mobile communications, and include radio resource management, cross-layer design and optimization, design and analysis of multiple antenna (MIMO) systems, cognitive and cooperative transmission techniques, performance evaluation, and energy efficiency, with a focus on Cellular, Ad Hoc, and Cognitive Radio networks.

Dr. Aïssa is the Founding Chair of the IEEE Women in Engineering Affinity Group in Montreal, 2004-2007; acted or is currently acting as TPC Leading Chair or Cochair of the Wireless Communications Symposium at IEEE ICC in 2006, 2009, 2011 and 2012; PHY/MAC Program Cochair of the 2007 IEEE WCNC; TPC Cochair of the 2013 IEEE VTC-spring; and TPC Symposia Cochair of the 2014 IEEE Globecom. Her main editorial activities include: Editor, IEEE TRANSACTIONS ON WIRELESS COMMUNICATIONS, 2004-2012; Technical Editor, IEEE WIRELESS COMMUNICATIONS MAGAZINE, 2006-2010; and Associate Editor, *Wiley Security and Communication Networks Journal*, 2007-2012. She currently serves as Technical Editor for the IEEE COMMUNICATIONS MAGAZINE. Awards to her credit include the NSERC University Faculty Award in 1999; the Quebec Government FQRNT Strategic Faculty Fellowship in 2001-2006; the INRS-EMT Performance Award multiple times since 2004, for outstanding achievements in research, teaching and service; and the Technical Community Service Award from the FQRNT Centre for Advanced Systems and Technologies in Communications in 2007. She is co-recipient of five IEEE Best Paper Awards and of the 2012 IEICE Best Paper Award; and recipient of NSERC Discovery Accelerator Supplement Award. She is a Distinguished Lecturer of the IEEE Communications Society (ComSoc) and an Elected Member of the ComSoc Board of Governors.

Ghassane Aniba (S'03-M'10) received the Ph.D degree in telecommunications from Institut National de la Recherche Scientifique-Energy, Materials and Telecommunications (INRS-EMT), Montreal, Canada, in 2009, and the Dipl.-Ing. degree in telecommunication engineering from the Institut National des Postes et Télécommunications (INPT), Rabat, Morocco, in 2002. In 2010, after a post-doctoral position at King Abdullah University of Science and Technology (KAUST), KSA, he joined Ecole Mohammadia d'Ingénieurs (EMI), Rabat, Morocco, where he is currently an Assistant Professor in Electrical and Telecommunication Engineering. He was the chair of the cooperative techniques and relays session at the 20th International Conference on Telecommunications 2013. His current research interests include Smart Grids, traffic modelling in green cognitive networks, cooperative wireless networks and wireless sensor networks.